JOURNAL OF PROPULSION AND POWER
Vol. 22, No. 6, November–December 2006

Real Fluid Modeling of Multiphase Flows in Liquid Rocket Engine Combustors

Gary C. Cheng*
University of Alabama at Birmingham, Birmingham, Alabama 35294-4461
and
Richard Farmer†
SECA, Inc., Carson City, Nevada 89701-8613

DOI: 10.2514/1.17272

The characteristics of propellant mixing near the injector have a profound effect on liquid rocket engine performance. Injector element geometry and propellant momentum are the only parameters available to control such mixing. A multiphase flow combustion model utilizing propellant real-fluid properties was developed to predict the mixing and thermal environment created by element configurations. The multiphase model was incorporated into a mature computational fluid dynamics code that can be used to simulate the flowfield near the injector and to analyze the combustion chamber and nozzle wall heating. The validity of the present model and code was investigated by comparing predictions to test data for two liquid oxygen/gaseous hydrogen unielement shear coaxial injector and two cryogenic nitrogen jet injection experiments. These simulations and those of several other investigators were critically compared at the 2nd International Workshop on Rocket Combustion Modeling. Based on these comparisons, it appears that the present model is a good, computationally efficient approximation of liquid rocket injector flows for both subcritical and supercritical spray combustion.

Nomenclature

a = speed of sound of a multicomponent mixture
B_{ij} = coefficients of the thermal property polynomial for a given species
Cp = constant-pressure specific heat
D = diameter of the center tube in an injector element
$\mathcal{D}_p$ = inverse of the matrix of the coefficients of the convective terms in the finite-difference form of the momentum equations
H = real-fluid enthalpy of a given species
H_0 = ideal-gas enthalpy of a given species
O/F = oxidizer-fuel ratio in mass
p = static pressure
p' = pressure correction
p^n = pressure at the previous time step
p^{n+1} = pressure at the current time step
p_c = critical pressure of a given species
p_r = reduced pressure of a given species
R = gas constant
r = radial distance
T = temperature
T_c = critical temperature of a given species
T_r = reduced temperature
t = time
$\boldsymbol{V}^*$ = velocity at the immediate time step
$\boldsymbol{V}'$ = velocity correction
X = axial distance
Z_c = compressibility of a given species at the critical point
β_p = partial derivative of density with respect to pressure at constant temperature
γ = specific heat of a multicomponent mixture
ρ = density of a given species or mean density of a mixture
ρ^n = density at the previous time step
ρ^* = density at the immediate time step
ρ' = density correction
ρ_c = density of a given species at the critical point
ρ_r = reduced density of a given species

I. Introduction

LIQUID rocket injectors use individual elements to feed propellants into high pressure combustion chambers. To accurately predict the thrust generated and the internal thermal environment of the engine using computational fluid dynamic (CFD) methods, the degree of local mixing and the extent of the combustion reactions must be established. These conditions cannot be measured experimentally. For numerical simulations, boundary conditions must be established using the following: the thermodynamic state of the propellants exiting the individual elements, the flow rate of the propellants exiting the individual elements, the geometry of the wall, and the thermal structure of the wall. Validated simulations for prototype engines have not been achieved because injectors usually consist of many elements, and the physics of dense spray combustion is very complex. These investigators devised and sought validation for an engineering model which predicts the mixing efficiency of an injector based solely on its geometric configuration.

The major problem in simulating dense spray flames is that the droplet particle size and distributions created by the individual injector elements cannot be measured [1]. This means that postulated droplet cloud models resulting from initial droplet formation and mixing cannot be validated. The multiphase flow model presented herein is based on reasonable, albeit approximate, physics of dense spray combustion. Many rocket engine combustors operate at supercritical conditions; hence, even if droplets are present, they would be unstable [2]. Had the entering propellants been assumed gaseous, the local propellant density, enthalpy, and mixing conditions would be erroneously simulated. Yet, such simulation approaches have been used by the industry since the early 1960s [3]. The new multiphase flow model uses a mature CFD code for turbulent, reacting flow and approximates the heterogeneous dense spray with an homogeneous, real fluid. Thus, the local amount of liquid propellant is described in terms of the fluid quality. The model

Presented as Paper 0785 at the 40th AIAA Aerospace Sciences Meeting and Exhibit, Reno, NV, 14–17 January 2002; received 19 April 2005; accepted for publication 2 February 2006.

*Assistant Professor, Mechanical Engineering Department, BEC 257, 1530 3rd Avenue South.
†President, SECA, Inc., 571 Gary's Way.

was constructed assuming there was no velocity or thermal lag between the phases.

Although elaborate, detailed spray combustion models have been reported, the authors employed extreme simplifications so that a significant number of injector elements could be analyzed. Model complexity was limited to that which could be verified by experimental test data.

Validation data were sought for which detailed flowfield measurements were made for a typical injector or for a simple ensemble of injector elements. Such data were not found. The best available data were deemed to be the benchmark test cases for multiphase spray flows presented by the 2nd International Workshop on Rocket Combustion Modeling (IWRCM) committee [4–6]. The intent of the workshop was to identify future needs in understanding spray combustion of cryogenic propellants by critically evaluating current CFD tools including the physical models imbedded in the codes. Four test cases were chosen for study at this workshop: subcritical single-element liquid oxygen (LOX)/gaseous hydrogen (GH_2) combustion, supercritical single-element LOX/GH_2 combustion, transcritical nitrogen cold flow, and supercritical nitrogen cold flow. The plan was to provide modelers with flow conditions and test configurations so that their simulations could be evaluated against test data at the workshop. It was not a completely blind comparison, as some of the participants conducted both the experiments and modeled the results. The test results were not available to the authors of this paper before the workshop.

The multiphase CFD combustion model with real-fluid dense spray properties and simulations made with this model for the IWRCM test cases are described as follows.

II. The Multiphase Flow CFD Model

Because the primary requirement of the spray combustion model is to predict local mixture concentrations and mass flow rates as a function of complex injector configurations, the simplest model that provides such information was considered first. An homogeneous multiphase approach treats liquid, gas, and dense fluids as coexisting continua and assumes there are no thermal and velocity lags between phases. This approach avoids modeling drop size and calculating droplet trajectories. Mass, momentum, and energy transport are modeled by both convection and diffusion processes, where the diffusion is controlled by viscosity and turbulence. The multiphase flow model is based on an accurate representation of the thermodynamic properties of propellant mixtures over the wide range of operating conditions existing in an engine.

Historically, heterogeneous models that track individual drops or clusters of droplets have been used to simulate spray flames [7,8]. However, geometry dependent submodels that initiate the droplet cloud and Euler/Lagrange tracking methods are needed to implement these models. Dense sprays have defied the identification and verification of the initiation submodels, and the tracking methodology has proven to be computationally intensive. Analyses reported with these methods do not spread the droplet cloud in a realistic fashion without additional tuning. Such tuning consists of specifying initial particle trajectories, size, and stripping rates. These parameters are not predictable functions of element geometry and flow rate; they must be determined empirically by testing the actual elements of interest. More recent work with droplet tracking [7,8] or with Eulerian/Eulerian particle/fluid interaction models [9] does not appear to mitigate the problems associated with heterogeneous models. Additional details of this point will be presented in the discussion of the RCM combustion test cases.

Spray combustion near the injector face is multiphase, reacting, and strongly striated. The spray flow can be subcritical and supercritical depending on the operating conditions. For subcritical sprays, surface tension and the heat of evaporation separate the phases and cause thermal and velocity lags. Droplets are atomized by velocity gradients between the liquid core and the surrounding gas, as well as by the turbulence. For dense sprays, the distinction between the liquid core and the droplet cloud becomes nebulous. On the other hand, for the supercritical spray the surface tension either does not exist or is not well defined, and, thus, the liquid droplets either are not present or are extremely unstable. Consequently, the liquid stream has a fluidlike behavior. This mixing characteristic was confirmed by several experimental studies [7,8]. All thermal and velocity lags are neglected in the multiphase flow model; hence, it remains to be shown that this neglect can be justified.

Mass, momentum, and energy transport are modeled by both convection and turbulent diffusion processes, with the finite-difference Navier–Stokes—real fluids version (FDNS-RFV) CFD code [10–13]. The FDNS-RFV CFD code is used to solve a set of coupled, nonlinear conservation equations. Finite differences were employed to discretize the equations on a nonstaggered grid. Second-order upwind differencing with fourth-order adaptive dissipation was used to represent convective terms in the present study. Second-order central differencing was used to represent viscous and source terms. Conjugate-gradient and generalized minimal residual matrix solvers were used to insure a stable, accurate, and fast convergence rate. Multiblock, multizone features were used to efficiently represent complex geometries. A pressure-based predictor/multi-corrector solution scheme was employed so that both compressible and incompressible flows could be simulated. Explicit time marching was used for these steady state simulations. Options to account for either finite-rate or equilibrium chemistry were used. Real-fluid properties are obtained from thermal and caloric equations of state. Favre-averaged Navier–Stokes equations with a two-equation k–ϵ model and wall functions were solved to account for the turbulence effects.

Real-fluid properties for the thermal and caloric equations of state, vapor pressure, heat of vaporization, surface tension, and transport properties are modeled with the equations of state (EOS) proposed by Hirschfelder et al. [14,15] (HBMS equations) and with conventional correlations [16]. The HBMS equations are convenient because arbitrary correlations for vapor pressure, heat of vaporization, and liquid densities can be used. A typical pressure-density-temperature correlation for a given species can be plotted as shown in Fig. 1, which consists of liquid, gas, two-phase, and dense fluid regimes. Multicomponent properties were predicted assuming the fluid was an ideal mixture. This assumption was necessary because of limited interaction correlations available for the wide range of species which were to be described. Both equilibrium and finite-rate combustion models were used to simulate the RCM combustion cases. A point implicit method was used to resolve the numerical stiffness associated with fast rate chemistry. The real-fluid property model was incorporated into the CFD solver.

HBMS thermal equation of state:

$$\frac{p}{p_c} = \sum_{j=1}^{4} T_r^{j-2} \sum_{i=1}^{6} B_{ij} \rho_r^{i-2}; \qquad T_r \equiv \frac{T}{T_c}; \qquad \rho_r \equiv \frac{\rho}{\rho_c}$$

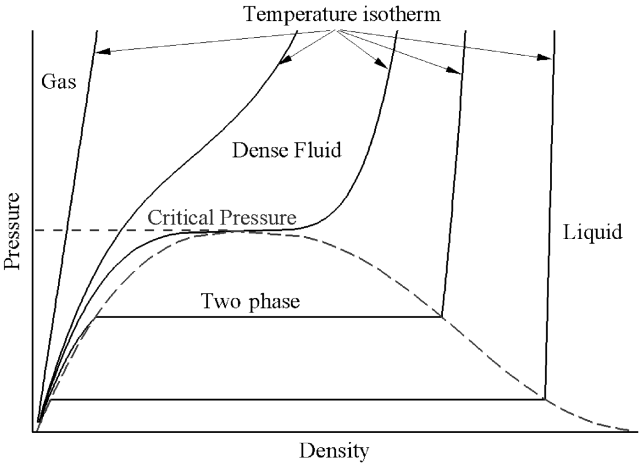

Fig. 1 Typical pressure-density-temperature correlation for a given species.

HBMS caloric equation of state:

$$\frac{H-H_0}{RT}=Z_c\int_0^{\rho_r}\left[\frac{p}{T_r}-\left(\frac{\partial p}{\partial T_r}\right)_{\rho_r}\right]\rho_r^{-2}\mathrm{d}\rho_r+Z_c\frac{p}{\rho_r T_r}-1$$

These equations are based on the "theorem of corresponding states," which states that the p–ρ–T relations for all species are similar if these variables are normalized with their values at the critical condition, that is, if reduced values are used. The real-fluid model was validated for O_2 and H_2 by comparing to the National Institute of Standards and Technology (NIST) database [17]. For a mixture under conditions where the species become ideal gases, the thermodynamic data from the chemical equilibrium composition (CEC) code [18] were used.

The FDNS-RFV code is a typical pressure-based code: a pressure correction (p') equation, derived from the continuity equation based on the ideal-gas laws, is solved to satisfy mass conservation. The pressure correction equation is expressed as

$$\frac{\beta_p p'}{\Delta t}+\nabla\cdot(\boldsymbol{V}^*\beta_p p')-\nabla\cdot(\rho^*\mathcal{D}_p\nabla p')=-\nabla\cdot(\rho^*\boldsymbol{V}^*)-\frac{\rho^*-\rho^n}{\Delta t}$$

$$p^{n+1}=p^n+p';\qquad \beta_p=1/RT;\qquad \boldsymbol{V}'\approx-\mathcal{D}_p\nabla p'$$

The pressure correction equation was modified to be applicable to multiphase flows. A correlation between pressure change and density change was used:

$$\rho'=\beta_p p'\quad\text{and}\quad\beta_p=\gamma/a^2$$

These properties were calculated with the real-fluid property submodel to account for variable density effects. As can be seen from the above correlation, the density becomes practically independent of pressure as fluids become liquid, and the speed of sound increases substantially as vapors condense. The above correlation is applied to the pressure correction equation to model the continuity equation for multiphase flow.

The multiphase flow model is very computationally efficient compared to droplet tracking approaches. However, the time step size for reacting flows is still limited due to the stiffness problem associated with calculating density and temperature based on the primitive variables, pressure and enthalpy, which are used in the thermodynamic properties submodel. Furthermore, the only justification for using the homogeneous model for subcritical spray combustion simulations is that it provides reasonable, computationally efficient simulations when compared to available test data.

III. The Multiphase Flow Model Validation

Test data presented at the 2nd IWRCM consisted of two cold flow cases of cryogenic nitrogen jets and two hot flow unielement jets of combusting LOX/GH_2, one subcritical (1.0 MPa) and the other supercritical (6.0 MPa). All four of these experiments were simulated to establish validation of the multiphase flow model.

The RCM-1-A and -B cold flow test cases [4] investigated the characteristics of a cryogenic, axisymmetric liquid nitrogen (LN_2) jet flowing into a stagnant environment. Case A is transcritical because the pressure of injection nitrogen was nearly equal to the critical pressure value; case B, though, is supercritical because the pressure was about twice the critical value. For both cases, the inlet temperature was approximately the critical value. Density profiles at various axial locations were measured using Raman scattering in a two-dimensional laser light sheet. Time-averaged density data were used for validation. The experiment was conducted with a single, nonreacting species such that the simulation model could be evaluated (in terms of fluid thermal properties and turbulent mixing) without the complexity of combustion.

RCM-2 [5] and -3 [6], LOX/GH_2 unielement shear coaxial injector test cases, were conducted to provide detailed flowfield measurements near the injector face. Most of the available data of liquid engine hot fire tests are global parameters such as chamber pressure, engine thrust, and heat flux to the nozzle wall. The importance of the RCM-2 and -3 test cases is that they provide temperature profiles and/or images of the hydroxyl radical near the injector element face. For the RCM-2 test case, the mean and standard deviation temperature measurements made with a coherent anti-Stokes Raman scattering (CARS) system were to be reported at several radial and axial stations. OH profiles were measured by laser-induced fluorescence (LIF) measurements and a subsequent Abel transformation for the RCM-2 and RCM-3 test cases. The operating conditions for these two cases are at high pressure (the RCM-2 case at 1.0 MPa which is below the oxygen critical pressure, and the RCM-3 case at 6.0 MPa which is slightly above this critical pressure). These two test cases provide appropriate validation for the multiphase real-fluid model under both subcritical and supercritical combustion conditions.

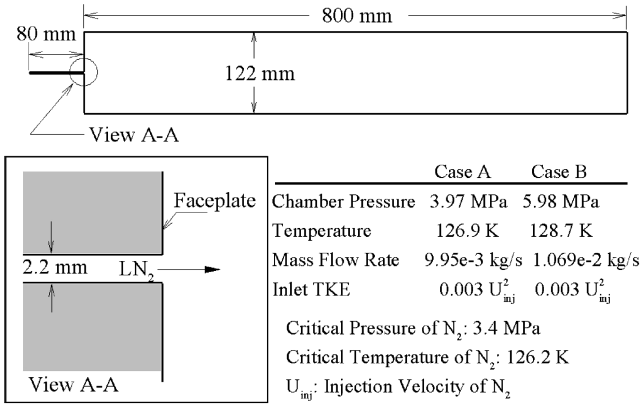

Fig. 2 Configuration and inlet flow conditions of the RCM-1-A and 1-B test cases.

The numerical simulations for both the RCM-2 and RCM-3 test cases were conducted with some simplification because complete detailed geometry information was unavailable [5,6]. These simplifications included the following. The flare of the LOX injector at the exit was neglected. The injector was assumed flush at the chamber head end instead of protruding into the chamber. The nozzle at the end of the combustion chamber was not included in the analyses. The wall coolant (later found to be helium) for the chamber was not included in the analyses because its flow rate and properties were not specified.

A. RCM-1 Test Case

The injector configuration and operating conditions for the cryogenic nitrogen jet of the RCM-1-A and 1-B test cases are presented in Fig. 2 and Table 1, respectively. Both test cases are axisymmetric cryogenic nitrogen (LN2) jet sprays into (case A) a transcritical pressure environment and into (case B) a supercritical pressure environment, relative to the critical pressure of nitrogen (3.4 MPa). A constant wall temperature was maintained in the RCM-1 experiments and was used as a boundary condition in the numerical simulation. A 101×11-mesh system was used to discretize the injector section, whereas the chamber section was modeled by a 301×101-mesh system for both the RCM-1 test cases. A finer mesh system (101×15 for the injector section and 301×141 for the chamber section) was used to simulate both case A and case B for a grid-sensitivity study. The results obtained by using both mesh

Table 1 RCM-1 test case operating conditions

Conditions	RCM-1-A	RCM-1-B
Chamber pressure	3.97 MPa	5.98 MPa
Temperature	126.9 K	128.7 K
Density	457.5 kg/m^3	514 kg/m^3
Mass flow rate	0.00995 kg/s	0.01069 kg/s
Velocity	0.769 m/s	0.736 m/s
Viscosity	28.8E-6 kg/m · s	35.8E-6 kg/m · s

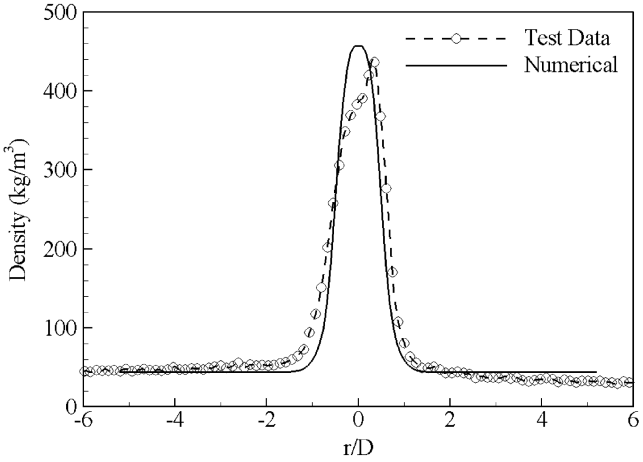

Fig. 3 Comparisons of density profile at $X/D = 5$, RCM-1-A test case.

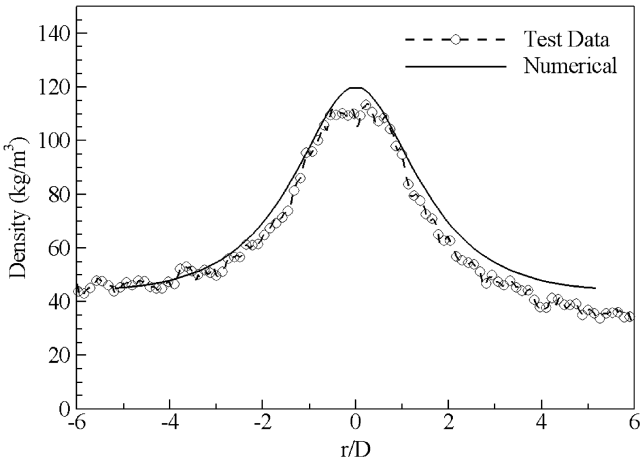

Fig. 4 Comparisons of density profile at $X/D = 25$, RCM-1-A test case.

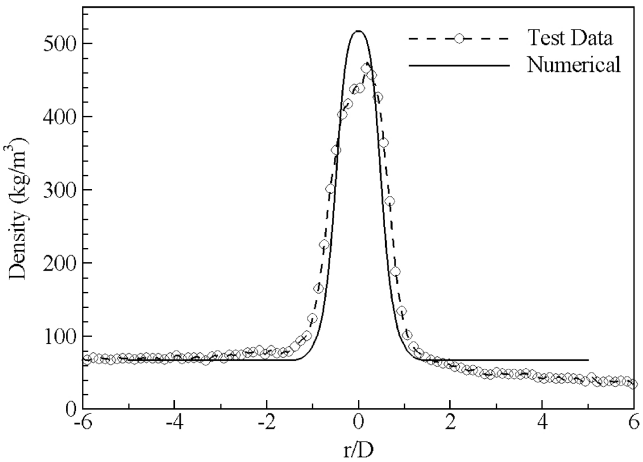

Fig. 5 Comparisons of density profile at $X/D = 5$, RCM-1-B test case.

systems were almost identical; therefore, only the coarse grid results are presented herein.

The numerical results of the RCM-1-A test case were compared to the available measurement at the axial locations of $X/D = 5$ and 25, and are plotted as shown in Figs. 3 and 4, respectively. Clearly, the multiphase flow model successfully predicts the width (spreading angle) of the cryogenic jet spray. Furthermore, the density profile predicted by the present model agrees quite well with the test data except for a slight discrepancy near the centerline of the jet. This

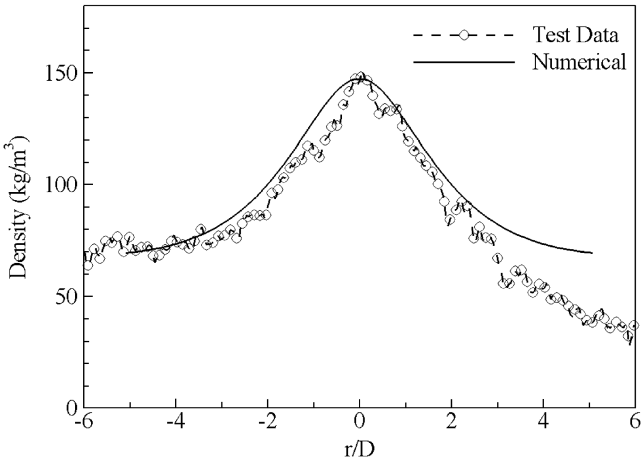

Fig. 6 Comparisons of density profile at $X/D = 25$, RCM-1-B test case.

result indicates that the homogeneous spray approach properly models the transport of liquid jets, and it also indicates that the real-fluid model accurately computes the thermal and state properties of the nitrogen. A minor discrepancy occurs where the test data exhibit some asymmetry near the density peak of the jet. It should be noted that axisymmetric assumption was used in the numerical simulation. Although no error bounds are estimated for the measurement data, obviously some error exists. This could be caused by optical reflection and refraction of the light sheet at the region of high densities. The observed small difference in the jet spray width indicates that the numerical model for turbulent mixing which controls the propellant diffusion in the multiphase flow model requires no adjustment.

The comparison between the numerical results and the test data of the RCM-1-B test case is shown in Figs. 5 and 6. The results are quite similar to the RCM-1-A test case. The agreement between the numerical simulation and experiment is generally good except near the density peak where some experimental errors may have occurred. This confirms that the multiphase CFD model is capable of simulating supercritical spray. Because the accuracy of the simulation and the test data appear to be comparable, tuning of the multiphase flow model is not required for either transcritical or supercritical dense sprays.

B. RCM-2 Test Case

The RCM-2 test case was designed to study the subcritical spray combustion from a unielement shear coaxial injector. The injector orifice diameter for the LOX injection is 5 mm surrounded by an annular GH_2 jet with an annular channel width of 3.2 mm. The overall O/F ratio for this case is 2.11. The test combustor cross section was 50 mm square although it was modeled as being circular. The operating conditions and injector configurations of the RCM-2 test case are illustrated in Table 2 and Fig. 7. Because the critical pressure of oxygen is 5.04 MPa and the test pressure was 1 MPa, this is a subcritical spray combustion test case. The inlet turbulent kinetic energy level and length scales shown in Fig. 7 for CFD simulations were proposed by the IWRCM organizers, so that all numerical

Table 2 RCM-2 test case operating conditions

Conditions	H_2	O_2
Chamber pressure	1 MPa	1 MPa
Mass flow rate	23.7 g/s	50 g/s
Temperature	287 K	85 K
Density	0.84 kg/m^3	1170 kg/m^3
Cp	14, 300 J/kg · K	1690 J/kg · K
Velocity	319 m/s	2.18 m/s
Viscosity	8.6E-6 kg/m · s	1.94E-4 kg/m · s
Surface tension	——	1.44E-2 N/m

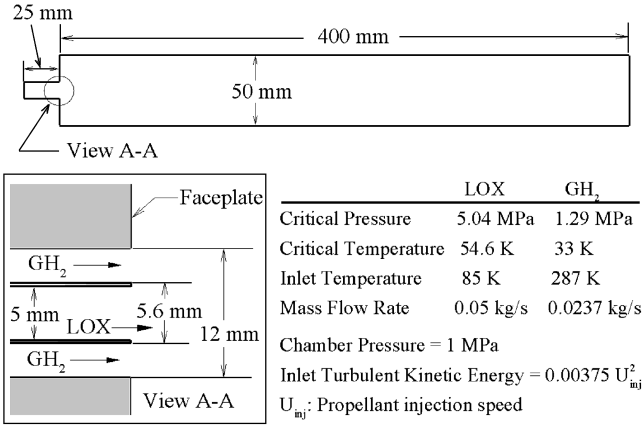

	LOX	GH_2
Critical Pressure	5.04 MPa	1.29 MPa
Critical Temperature	54.6 K	33 K
Inlet Temperature	85 K	287 K
Mass Flow Rate	0.05 kg/s	0.0237 kg/s

Chamber Pressure = 1 MPa

Inlet Turbulent Kinetic Energy = $0.00375\ U_{inj}^2$

U_{inj}: Propellant injection speed

Fig. 7 Configuration and inlet flow conditions of the RCM-2 test case.

results could be compared on a similar basis. Both equilibrium chemistry and finite-rate chemistry simulations were made to represent the combustion process. The H_2/O_2 kinetics model for combustion of hydrogen and oxygen to form H_2O, O, H, and OH used nine reactions with accepted values for their rate constants [19,20]. It should be noted that this multiphase flow combustion model makes no distinction between the reactivity of liquid and gaseous oxygen.

The grid used for the injector element was 61×43; for the chamber, it was 301×101. The nozzle was not modeled in the homogeneous spray simulation. This grid system had a minimum grid spacing of 60 μm in the wake behind the lip separating the LOX and hydrogen streams. A finer grid system (especially in both the LOX post region and the outer jet expansion region) was also employed for this case to study grid sensitivity. The finer grid system reduced the grid spacing for the LOX post from 60 to 30 μm. The simulated shear layer and the flame sheet became unsteady with the finer grid system. This flow unsteadiness could be caused by multiscale turbulence, combustion stability, multiphase fluid properties, numerics, and/or a combination of these factors.

Because RCM-2 is subcritical spray combustion, several droplet tracking simulations were presented at the IWRCM [21–23]. Droplet tracking methodology requires the specification of several parameters not required by the multiphase flow model. These include velocity, direction, and size (or size distribution) of the drops and a liquid core length. Correlations and empirical equations to describe these variables were proposed by the workshop organizers [5]. Three droplet tracking simulations [21–23] were presented using these proposed parameters and some variation of them.

Computed and measured radial temperature profiles are compared at four axial locations ($X = 10$, 180, 250, and 410 mm) as shown in Figs. 8–11. The comparisons of temperature distributions in the axial direction at two radial locations ($r/D = 2$, and 3) are shown in Figs. 12 and 13. It can be seen that the predicted temperatures generally correspond to test data, despite some discrepancies which occur at $X/D = 2$ and 36. The contours of calculated OH concentrations plotted in comparison with OH images from the experimental test are shown in Fig. 14. It is apparent that the characteristics of the shear layer, the primary indicator to assess the turbulent mixing and thermal properties, are accurately simulated by

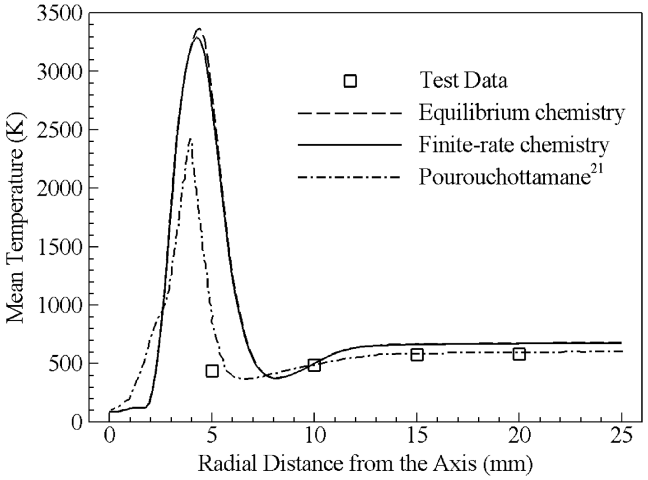

Fig. 8 Comparisons of temperature profile at $X/D = 2$, RCM-2 test case.

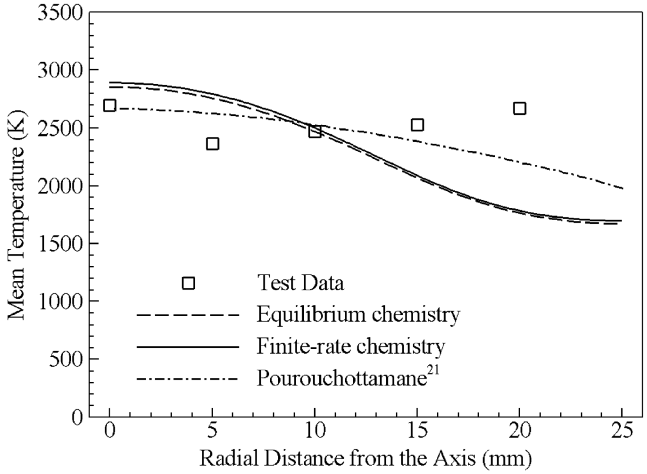

Fig. 9 Comparisons of temperature profile at $X/D = 36$, RCM-2 test case.

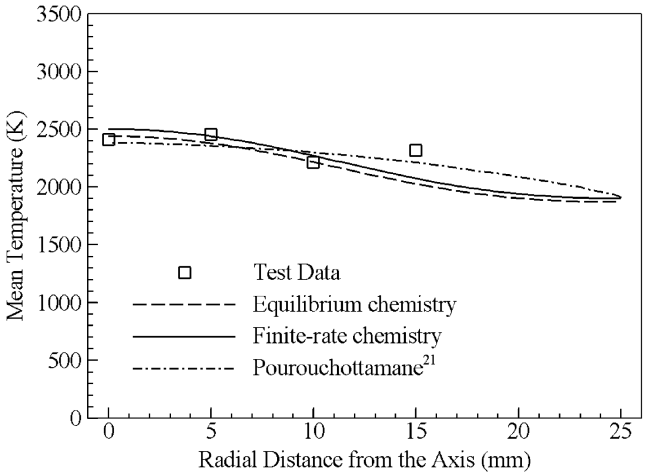

Fig. 10 Comparisons of temperature profile at $X/D = 50$, RCM-2 test case.

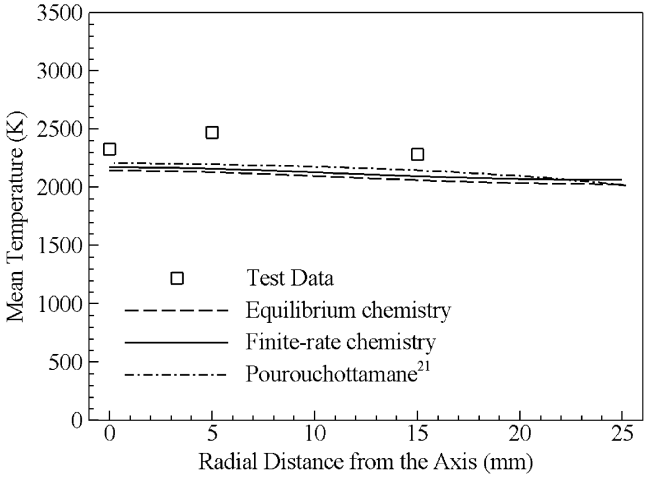

Fig. 11 Comparisons of temperature profile at $X/D = 82$, RCM-2 test case.

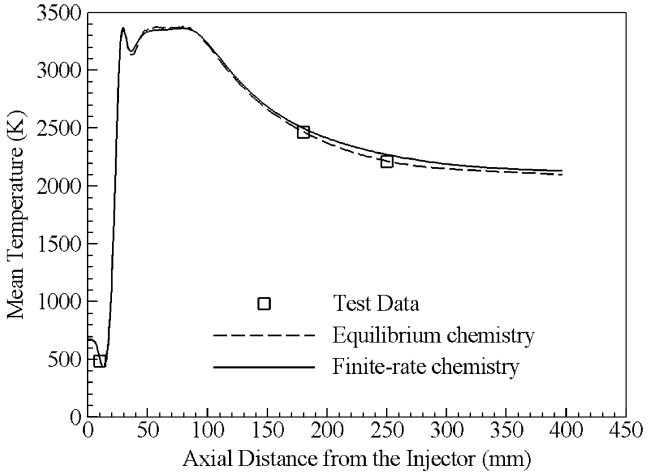

Fig. 12 Comparisons of temperature profile at $r/D = 2$, RCM-2 test case.

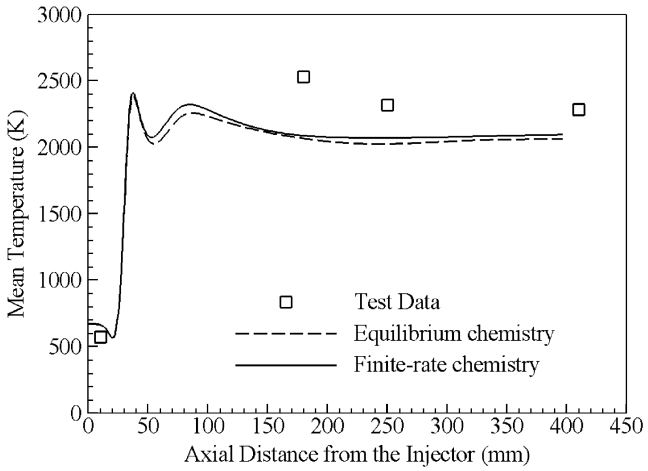

Fig. 13 Comparisons of temperature profile at $r/D = 3$, RCM-2 test case.

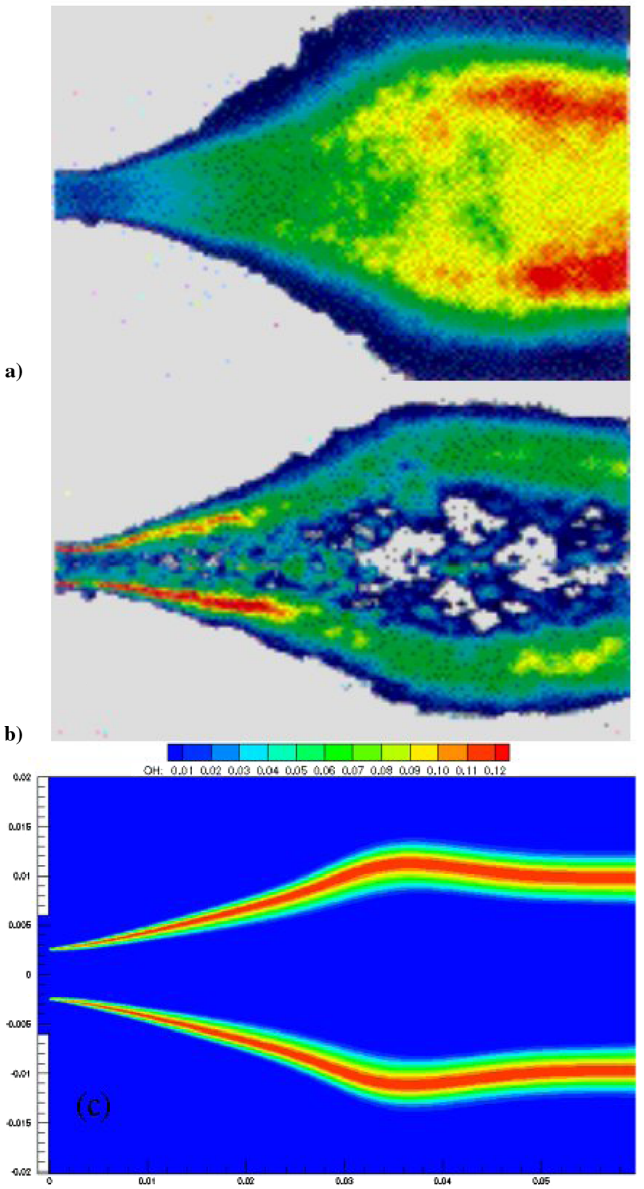

Fig. 14 Comparisons of OH concentrations, RCM-2 test case. a) Time-averaged emission, b) Abel transformed emission, and c) numerical results.

the present model. The reattachment lengths predicted by the droplet tracking methods were about 5 cm from the injector face; the multiphase flow model prediction was about 4 cm. These lengths are approximate because they were read from small scale temperature plots of the simulation results. More important, the numerical results of the present model are compared to the predicted data from [21] for the radial temperature profiles at various axial stations. These comparisons are shown in Figs. 8–11. The agreement between the simulations is remarkable.

The equilibrium chemistry and chemical kinetics simulations are almost identical because the H_2/O_2 reactions are extremely fast at this high pressure condition. The minor effect of rate chemistry can only be seen at the region very close to the injector tip where the flow's residence time is extremely short.

The biggest discrepancies between measurement and prediction occur at $X/D = 2$ and 36 (Figs. 8 and 9) and are explained as follows. In Fig. 8, the test data show no temperature spike at $X/D = 2$ (near the injector tip), whereas both the present model and the droplet tracking model [21] show a temperature spike in the shear layer region. Hence, we believe the absent temperature spike in the test data may be caused by lacking spatial resolution in the CARS measurement, as can be seen from the distance between data points in Fig. 8. However, the present method and the droplet tracking method [21] predicted different magnitude and width of the temperature spike. This discrepancy can be attributed to the thermal equilibrium assumption used in the multiphase flow model. With the approximation of neglecting the heat transfer lag between the liquid droplet and its surrounding gases, which can be important in the subcritical spray depending on the species involved, the multiphase flow model may overpredict the amount of oxygen available for combustion, which leads to locally higher temperature and larger expansion effect in the shear layer. However, there were insufficient test data to validate which method is more accurate.

In Fig. 9, the disagreement at $X/D = 36$ occurs in the region towards the wall (in a fuel-rich region outside of the shear layer), where the test data indicate higher temperatures than in the shear layer. The fuel-rich region near the wall should be cooler than the shear layer, not hotter. It is suspected that measurement errors in the test data cause this discrepancy. In Fig. 9, the droplet tracking method predicted a similar trend to the present method. Such similarity supports the previous assessment of measurement errors as being the cause of the discrepancy. This figure and its interpretation are shown to illustrate the need for improving the accuracy of the test data.

A further simulation using the droplet tracking methodology of the RCM-2 case was also reported in [24]. This simulation did not use the droplet parameters suggested by the workshop organizers; rather, only initial drop size was used. This simulation resulted in a very narrow jet which never reattached to the combustor wall. It is reasonable to assume that the parameter correlations suggested by

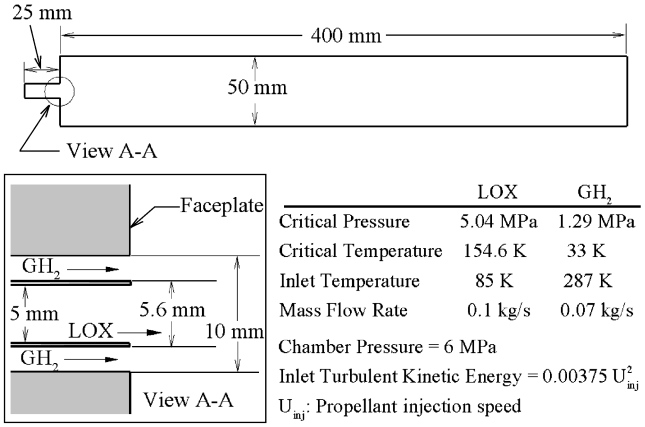

	LOX	GH_2
Critical Pressure	5.04 MPa	1.29 MPa
Critical Temperature	154.6 K	33 K
Inlet Temperature	85 K	287 K
Mass Flow Rate	0.1 kg/s	0.07 kg/s

Chamber Pressure = 6 MPa

Inlet Turbulent Kinetic Energy = $0.00375\ U_{inj}^2$

U_{inj}: Propellant injection speed

Fig. 15 Configuration and inlet flow conditions of the RCM-3 test cases.

the workshop organizers were developed for the RCM-2 test case, or at least from very similar experiments, because the modelers and experimenters were from the same organization. In any event, the generality of the droplet tracking parameters is unknown.

Despite the fact that there are some discrepancies between both simulations and the measurements near the injector face, both models represent the subcritical spray combustion case fairly well. Because the present multiphase model is more computationally efficient and requires no empirical droplet parameters, it should be seriously considered for further development. Without more accurate test data and data from more critical locations the absolute accuracy of model simulations cannot be determined.

C. RCM-3 Test Case

The injector configuration and flow conditions for the supercritical combustion RCM-3 test case are presented in Fig. 15 and Table 3. The dimensions of the LOX orifice, annulus width, and chamber diameter are the same as those of the RCM-2 test case. The operating conditions of the RCM-3 test case are given in Table 3. The high chamber pressure indicates that this case is supercritical. Just as with the RCM-2 test case, the inlet turbulent kinetic energy level and length scale employed in the CFD simulation were specified by the IWRCM organizers. A two-zone mesh system (61×39 and 301×101) was used to model the injector section and the combustion chamber. A grid-sensitivity study was conducted with a finer grid system (especially in both the LOX post region and the outer jet expansion region). Similar to the RCM-2 test case, the numerical results of the fine grid system exhibited unsteady flow behavior (both the shear layer and the flame sheet oscillated) and, thus, are not included in this paper.

As shown in the RCM-2 test case, the effect of rate chemistry on the H_2/O_2 combustion at elevated pressure is almost negligible in the chamber region; consequently, only the results of equilibrium chemistry are reported herein. The radial temperature profiles predicted at several axial stations are shown in Fig. 16, and the axial temperature profiles at several radial locations are shown in Fig. 17. The contours of predicted temperature and oxygen and OH concentrations are shown in Fig. 18.

Table 3 RCM-3 test case operating conditions

Conditions	H_2	O_2
Chamber pressure	6 MPa	6 MPa
Mass flow rate	70 g/s	100 g/s
Temperature	287 K	85 K
Density	5.51 kg/m^3	1177.8 kg/m^3
Cp	15100 J/kg · K	1660.9 J/kg · K
Velocity	236 m/s	4.35 m/s
Viscosity	8.67E-6 kg/m · s	12.34E-4 kg/m · s

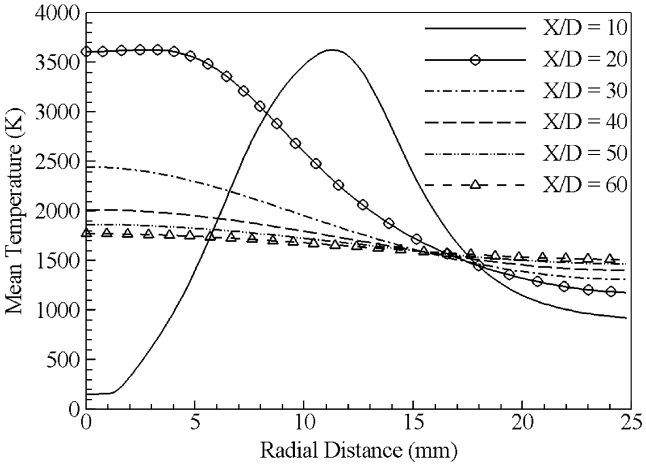

Fig. 16 Radial temperature profiles at various axial locations, RCM-3 test case.

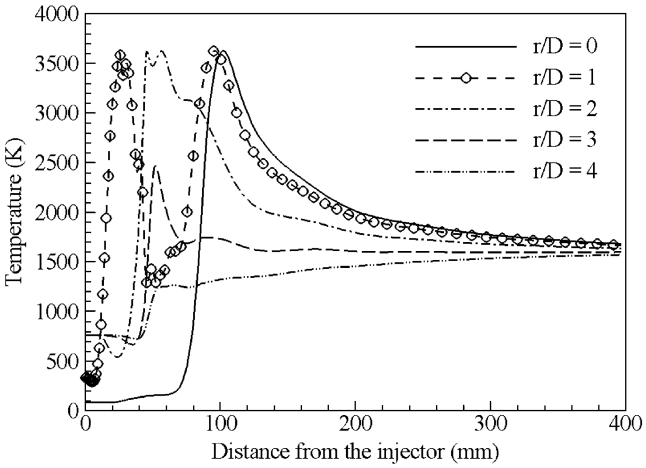

Fig. 17 Axial temperature profiles at various radial locations, RCM-3 test case.

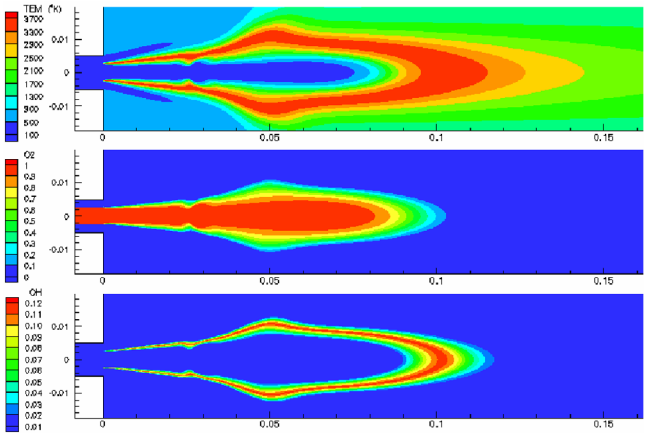

Fig. 18 Temperature, O_2 and OH concentrations near the injector face, RCM-3 test case.

Unfortunately, there are no temperature data available to validate these numerical results. Only the LIF image of the hydroxyl radical, OH, from the experiment is available for verification. The comparison of OH concentrations near the injector is illustrated in Fig. 19. It should be noted that a scale is not given for the LIF data. Qualitatively, the predicted flame zone and expansion angle of the shear layer very closely correspond to those of the OH images. Because the flame location and expansion angle are determined by

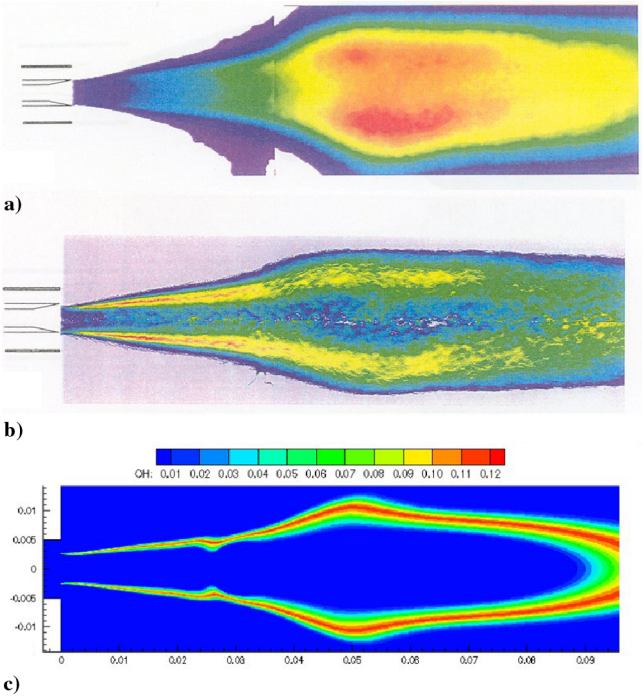

Fig. 19 Comparisons of OH concentrations, RCM-3 test case. a) Time-averaged emission, b) Abel transformed emission, and c) numerical results.

the mixing and reaction of propellants, the qualitative similarity indicates that the multiphase flow model reasonably predicts the turbulence mixing and thermal properties. The multiphase flow model is, therefore, capable of simulating the supercritical spray combustion flow. Other simulations presented at the IWRCM workshop were not successful in predicting the flame zone and underpredicted the expansion angle of the propellant. In fact, Legrand et al. [25] conclude, "It appears that a real gas law for oxygen should be interesting for (it) eliminates all the problems relative to droplet injection." Detailed test data, such as temperature profiles, are needed to completely validate the multiphase supercritical flow model.

IV. Conclusions

A multiphase flow, real-fluid spray combustion model was postulated and validated by comparison to pertinent test data. The evaluation showed that the model was reasonable and that no modifications are needed to account for multiphase thermal lags or turbulent mixing effects. Even though the simulations were computationally intensive, the chamber mixing and local heat release in terms of injector design parameters were predictable. Improvements to the computational efficiency are currently being addressed. More important, testing parameters (such as the location of temperature measurements) can now be identified that, when measured, can lead to improved simulation methodology.

The validity of the multiphase flow model was established by simulating several benchmark experiments. The spray angle and thermal properties of both transcritical and supercritical cryogenic nitrogen flows were accurately predicted. The model also quantitatively predicts the spray angle and flame zone for subcritical and supercritical spray combustion of single LOX/GH_2 shear coaxial injector element flows.

The multiphase flow model simulates the essential flow characteristics and underlying physics of dense spray combustion, specifically the thermal properties of liquid species and the mixing between propellants. The model, therefore, serves the desired purpose of relating injector element configurations to delivered mixture ratios in a rocket engine combustor.

Acknowledgements

This work was performed under NAS8-00162 for the Marshall Space Flight Center of the National Aeronautics and Space Administration. The authors wish to thank the organizers of the 2nd IWRCM meeting for sharing their test data and providing the forum for discussing such tests. The authors also wish to express their appreciation to John Hutt, Robert Garcia, and Bill Anderson for their encouragement and support. Valuable suggestions from Kevin Tucker and Jeff West in revising this paper are deeply appreciated.

References

[1] Sutton, R. B., Schuman, M. D., and Chadwick, W. D., "Operating Manual for Coaxial Injection Combustion Model," NASA CR-129031, Rocketdyne Division, Rockwell International, Canoga Park, CA, April 1974.

[2] Mayer, W., and Tamura, H., "Flow Visualization of Supercritical Propellant Injection in a Firing LOX/GH2 Rocket Engine," AIAA Paper 95-2433, 1995.

[3] Nickerson, G. R., Coats, D. E., Dang, A. L., Dunn, S. S., and Kehtarnavaz, H., "Two-Dimensional Kinetics (TDK) Nozzle Performance Computer Program," Vols. 1–3, Rept. SN91, Software and Engineering Associates, Inc., March 1989.

[4] Telaar, J., Schneider, G., Hussong, J., and Mayer, W., "Cryogenic Jet Injection: Description of Test Case RCM 1," *Proceedings of the 2nd International Workshop on Rocket Combustion Modeling*, Deutsches Zentrum fur Luft-und Raumfahrt (DLR), Lampoldshausen, Germany, 2001.

[5] Vingert, L., and Habiballah, M., "Test Case RCM 2: Cryogenic Spray Combustion at 10 bar at Mascotte," *Proceedings of the 2nd International Workshop on Rocket Combustion Modeling*, Deutsches Zentrum fur Luft-und Raumfahrt (DLR), Lampoldshausen, Germany, 2001.

[6] Thomas, J. L., and Zurbach, S., "Test Case RCM 3: Supercritical Spray Combustion at 60 bar at Mascotte," *Proceedings of the 2nd International Workshop on Rocket Combustion Modeling*, Deutsches Zentrum fur Luft-und Raumfahrt (DLR), Lampoldshausen, Germany, 2001.

[7] Chiang, C. H., and Sirignano, W. A., "Axisymmetric Vaporizing Oxygen Droplet Computations," AIAA Paper 91-0281, 1991.

[8] Shuen, J. S., and Yang, V., "Combustion of Liquid-Fuel Droplets in Supercritical Conditions," AIAA Paper 91-0078, 1991.

[9] van Wachem, B. G. M., Schouten, J. C., van den Bleek, C. M., Krishna, R., and Sinclair, J. L., "Comparative Analysis of CFD Models of Dense Gas-Solid Systems," *AIChE Journal*, Vol. 47, May 2001, pp. 1035–1051.

[10] Chen, Y. S., "Compressible and Incompressible Flow Computations with a Pressure Based Method," AIAA Paper 89-0286, 1989.

[11] Cheng, G.,C., Chen, Y. S., Garcia, R., and Williams, R. W., "Numerical Study of 3-D Inducer and Impeller for Pump Model Development," AIAA Paper 93-3003, 1993.

[12] Cheng, G. C., Farmer, R. C., and Chen, Y. S., "Numerical Study of Turbulent Flows with Compressibility Effects and Chemical Reactions," AIAA Paper 94-2026, 1994.

[13] Cheng, G. C., Anderson, P. G., and Farmer, R. C., "Development of CFD Model for Simulating Gas/Liquid Injectors in Rocket Engine Design," AIAA Paper 97-3228, 1997.

[14] Hirschfelder, J. O., Buehler, B. J., McGee, H. A., Jr., and Sutton, J. R., "Generalized Equations of State for Gases and Liquids," *Industrial and Engineering Chemistry*, Vol. 50, No. 3, 1958, pp. 375–385.

[15] Hirschfelder, J. O., Buehler, B. J., McGee, H. A., Jr., and Sutton, J. R., "Generalized Excess Functions for Gases and Liquids," *Industrial and Engineering Chemistry*, Vol. 50, No. 3, 1958, pp. 386–390.

[16] Reid, R. C., Praunitz, J. M., and Poling, B. E., *The Properties of Gases & Liquids*, 4th ed., McGraw–Hill, New York, 1987.

[17] NIST Chemistry WebBook, NIST Standard Database No. 69, June 2005 Release, http://webbook.nist.gov/chemistry.

[18] Gordon, S., and McBride, B. J., "Computer Program for Calculation of Complex Chemical Equilibrium Compositions, Rocket Performance, Incident and Reflected Shocks, and Chapman-Jouget Detonations," NASA-SP-273, 1971, and SP-273, Interim Revision, 1976.

[19] Edelman, R. B., and Harsha, P. T., "Laminar and Turbulent Gas Dynamics in Combustors-Current Status," *Progress in Engineering and Combustion Science*, Vol. 4, No. 1, 1978, pp. 1–6.

[20] Gardiner, W. C., Jr., *Combustion Chemistry*, Springer–Verlg, New York, 1984.

[21] Pourouchottamane, M., Burnley, V., Dupoirieux, F., and Habiballah, M., "Numerical Analysis of the 10 bar Mascotte Flow Field,"

Proceedings of the 2nd International Workshop on Rocket Combustion Modeling, Deutsches Zentrum fur Luft-und Raumfahrt (DLR), Lampoldshausen, Germany, 2001.

[22] Bodele, E., Gökalp, I., Zurbach, S., and Saucereau, D., "Modeling of Mascotte 10 bar Case with THESEE Code with and Without a Secondary Atomization Model," *Proceedings of the 2nd International Workshop on Rocket Combustion Modeling*, Deutsches Zentrum fur Luft-und Raumfahrt (DLR), Lampoldshausen, Germany, 2001.

[23] Blouquin, R., and Lequette, L., "Combustion of Cryogenic Propellant at 10 bars Using the CPS Code," *Proceedings of the 2nd International Workshop on Rocket Combustion Modeling*, Deutsches Zentrum fur Luft-und Raumfahrt (DLR), Lampoldshausen, Germany, 2001.

[24] Farmer, R. C., Cheng, G. C., and Chen, Y. S., "CFD Simulation of Liquid Rocket Engine Injectors: Test Case RCM 3," *Proceedings of the 2nd International Workshop on Rocket Combustion Modeling*, Deutsches Zentrum fur Luft-und Raumfahrt (DLR), Lampoldshausen, Germany, 2001.

[25] Legrand, B., Durand, P., and Vuillermoz, P., "Test Case RCM-3 Using CPS," *Proceedings of the 2nd International Workshop on Rocket Combustion Modeling*, Deutsches Zentrum fur Luft-und Raumfahrt (DLR), Lampoldshausen, Germany, 2001.

J. Oefelein
Associate Editor